

Genetically designed biomolecular capping system for mesoporous silica nanoparticles enables receptor-mediated cell uptake and controlled drug release

Stefan Datz, Christian Argyo, Michael Gattner, Veronika Weiss, Korbinian Brunner, Johanna Bretzler, Constantin von Schirnding, Adriano Torrano, Fabio Spada, Milan Vrabel[§], Hanna Engelke, Christoph Bräuchle, Thomas Carell, and Thomas Bein*

*Department of Chemistry, Nanosystems Initiative Munich (NIM), Center for Nano Science (CeNS), and Center for Integrated Protein Science Munich (CIPSM), University of Munich (LMU), Butenandtstr. 5-13, 81377 Munich, Germany. [§]Institute of Organic Chemistry and Biochemistry, Academy of Sciences of the Czech Republic, *E-mail:bein@lmu.de.*

Experimental Details

Materials. Tetraethyl orthosilicate (TEOS, Fluka, > 99 %), triethanolamine (TEA, Aldrich, 98 %), cetyltrimethylammonium chloride (CTAC, Fluka, 25 % in H₂O), (3-mercaptopropyl)-triethoxysilane (MPTES, Sigma Aldrich, > 80 %), 6-maleimidohexanoic acid *N*-hydroxysuccinimide ester (Fluka, > 98 %), bovine carbonic anhydrase (bCA, Sigma, > 95 %), 4-(2-aminoethyl)benzenesulfonic acid (Aldrich, 98 %), folic acid (FA, Sigma Aldrich, ≥ 97 %), 4,6-Diamidino-2-phenylindole dihydrochloride (DAPI, Sigma-Aldrich, ≥ 98 %), CellEvent™ Caspase-3/7 Green Detection Reagent (lifeTechnologies), Hoechst 33342, Trihydrochloride, Trihydrate (lifeTechnologies), Wheat Germ Agglutinin, Alexa Fluor® 488 Conjugate (lifeTechnologies), CellLight© Early Endosome-GFP, Late Endosome-GFP, and Lysosome-GFP, BacMam 2.0 (lifeTechnologies), Atto 633 maleimide (ATTO-TEC), ammonium nitrate (NH₄NO₃, Aldrich), ammonium fluoride (NH₄F, Aldrich), hydrochloric acid (37 %), fluorescein disodium salt dihydrate (Aldrich, 90 %), and Hank's balanced salt solution (HBSS-buffer, Sigma Aldrich) were

used as received. Ethanol (EtOH, absolute, Aldrich), DMSO and dimethylformamide (DMF, dry, Aldrich) were used as solvent without further purification. Bidistilled water was obtained from a millipore system (Milli-Q Academic A10). Citric-acid phosphate buffer (CAP-buffer, pH 5.5) was freshly prepared by carefully mixing a certain amount of disodium hydrogen phosphate (Na_2HPO_4 , 0.2 M in H_2O) and citric acid (0.2 M in H_2O) to adjust a pH value of 5.5. Subsequently, the solution was diluted with bidistilled H_2O to a total volume of 500 mL.

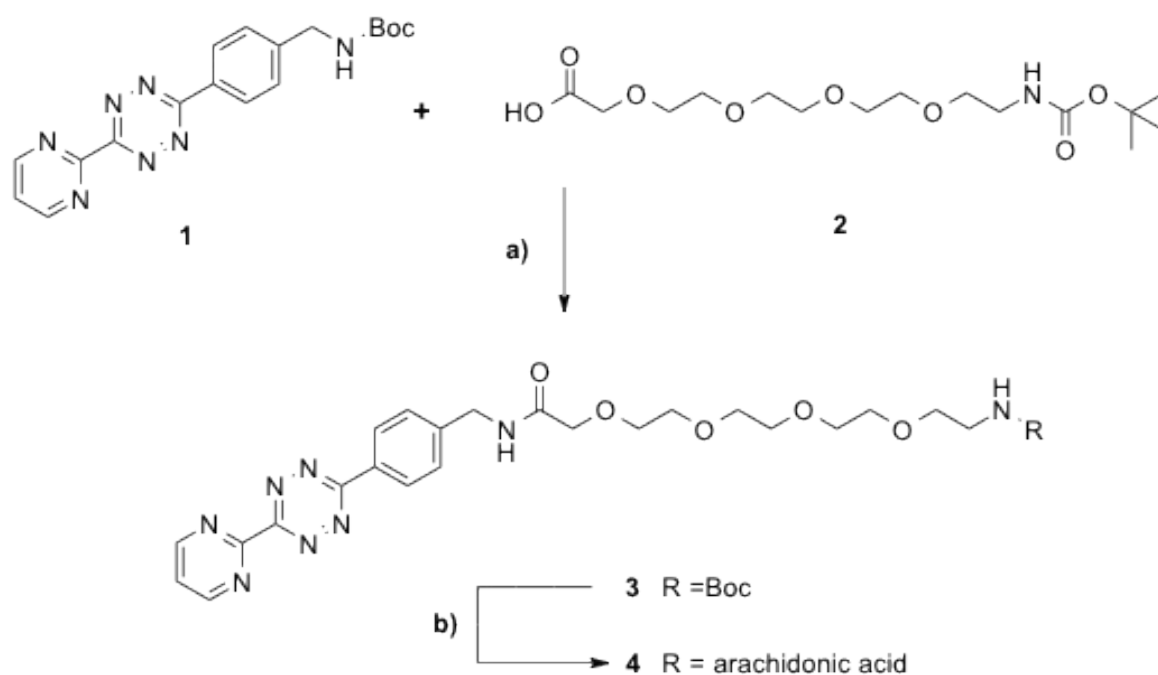
Characterization. DLS and zeta potential measurements were performed on a Malvern Zetasizer Nano instrument equipped with a 4 mW He-Ne-Laser (633 nm) and an avalanche photodiode detector. DLS measurements were directly recorded in diluted colloidal suspensions of the particles at a concentration of 1 mg/mL. Zeta potential measurements were performed using the add-on Zetasizer titration system (MPT-2) based on diluted NaOH and HCl as titrants. For this purpose, 1 mg of the particles was diluted in 10 mL bi-distilled water. Thermogravimetric analyses (TGA) of the bulk extracted samples (approximately 10 mg) were recorded on a Netzsch STA 440 C TG/DSC. The measurements proceeded at a heating rate of 10 °C/min up to 900 °C in a stream of synthetic air of about 25 mL/min. Nitrogen sorption measurements were performed on a Quantachrome Instrument NOVA 4000e at -196 °C. Sample outgassing was performed for 12 hours at a vacuum of 10 mTorr at RT. Pore size and pore volume were calculated by a NLDFT equilibrium model of N_2 on silica, based on the desorption branch of the isotherms. In order to remove the contribution of the interparticle textural porosity, pore volumes were calculated only up to a pore size of 8 nm. A BET model was applied in the range of 0.05 – 0.20 p/p_0 to evaluate the specific surface area. Infrared spectra of dried sample powder were recorded on a ThermoScientific Nicolet iN10 IR-microscope in reflexion-absorption mode

with a liquid-N₂ cooled MCT-A detector. Raman spectroscopy measurements were performed on a confocal LabRAM HR UV/VIS (HORIBA Jobin Yvon) Raman microscope (Olympus BX 41) with a SYMPHONY CCD detection system. Measurements were performed with a laser power of 10 mW at a wavelength of 633 nm (HeNe laser). Dried sample powder was directly measured on a coverslip. UV/VIS measurements were performed on a Perkin Elmer Lambda 1050 spectrophotometer equipped with a deuterium arc lamp (UV region) and a tungsten filament (visible range). The detector was an InGaAs integrating sphere. Fluorescence spectra were recorded on a PTI spectrofluorometer equipped with a xenon short arc lamp (UXL-75XE USHIO) and a photomultiplier detection system (model 810/814). The measurements were performed in HBSS buffer solution at 37 °C to simulate human body temperature. For time-based release experiments of fluorescein a custom made container consisting of a Teflon tube, a dialysis membrane (ROTH Visking type 8/32, MWCO 14,000 g/mol) and a fluorescence cuvette was used. The excitation wavelength was set to $\lambda = 495$ nm for fluorescein-loaded MSNs. Emission scans (505 – 650 nm) were performed every 5 min. All slits were adjusted to 1.0 mm, bandwidth 8 nm). Mass spectra were recorded a *Thermo LTQ-Orbitrap XL*. For analytical HPLC separations of protein and peptide samples with subsequent MS a *Dionex Ultimate 3000 Nano* HPLC was used. Acetonitrile of LC-MS grade was purchased from *Carl Roth GmbH + Co. KG*. Water was purified by a Milli-Q Plus system from *Merck Millipore*.

Synthesis of Anandamide-tetrazine

Chemicals were purchased from *Sigma-Aldrich*, *Fluka* or *Acros* and used without further purification. Solutions were concentrated *in vacuo* on a *Heidolph* rotary evaporator. The solvents were of reagent grade and purified by distillation. Chromatographic purification of

products was accomplished using flash column chromatography on *Merck Geduran Si 60* (40-63 μM) silica gel (normal phase). Thin layer chromatography (TLC) was performed on *Merck 60* (silica gel F254) plates. Visualization of the developed chromatogram was performed using fluorescence quenching or staining solutions. ^1H and ^{13}C NMR spectra were recorded in deuterated solvents on *Bruker ARX 300*, *Varian VXR400S*, *Varian Inova 400* and *Bruker AMX 600* spectrometers and calibrated to the residual solvent peak. Multiplicities are abbreviated as follows: s = singlet, d = doublet, t = triplet, q = quartet, m = multiplet, br. = broad. ESI spectra and high-resolution ESI spectra were obtained on the mass spectrometers *Thermo Finnigan LTQ FT-ICR*. IR measurements were performed on *Perkin Elmer Spectrum BX FT-IR* spectrometer (Perkin Elmer) with a diamond-ATR (Attenuated Total Reflection) setup. Repetencies are given in cm^{-1} . The intensities are abbreviated as follows: vs (very strong), s (strong), m (medium), w (weak), vw (very weak).



After 10 min the deprotected tetrazinamine (0.068 mg, 0.260 mmol, 1 eq.) was added and the reaction was stirred over night at RT. The reaction was diluted with DCM and the washed with water and brine before the combined organic phases were dried over MgSO_4 and the solvent was removed *in vacuo*. The residue was purified by column chromatography (silica, DCM/EtOAc/MeOH, 5:5:1) to obtain the **3** as violet oil (66.0 mg, 0.110 mmol, 42%).

$R_f = 0.22$ ($\text{CH}_2\text{Cl}_2/\text{EtOAc}/\text{MeOH}$, 5:5:1).

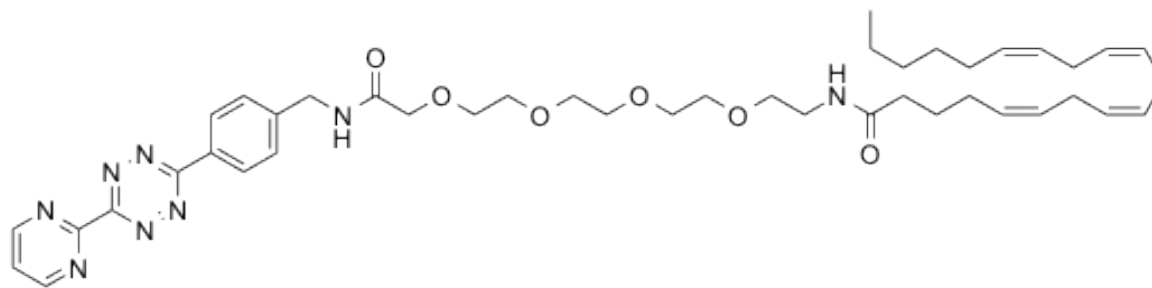
$^1\text{H-NMR}$ (600 MHz, CDCl_3): δ [ppm] = 9.11 (d, $^3J = 4.9$ Hz, 2H, $2\times\text{C-H}_{\text{arom}}$), 8.68 (d, $^3J = 8.4$ Hz, 2H, $2\times\text{C-H}_{\text{arom}}$), 7.59 – 7.54 (m, 1H, C-H_{arom}), 4.61 (d, $^3J = 6.2$ Hz, 2H, $\text{Ar-CH}_2\text{-NH}$), 4.12 – 4.08 (m, 2H, $\text{C=O-CH}_2\text{-O}$), 3.73 – 3.50 (m, 14H, tetraethylene glycol $7\times\text{CH}_2$), 3.47 (t, $^3J = 5.1$ Hz, 2H, $\text{CH}_2\text{-NH}$), 1.40 (s, 9H, $3\times\text{CH}_3\text{-tBu}$).

$^{13}\text{C-NMR}$ (150 MHz, CDCl_3): δ [ppm] = 164.57, 163.32, 159.82, 159.81, 158.62, 129.33, 128.77, 122.68, 70.62, 70.36 (Tetraethylenglykol $7\times\text{CH}_2$), 42.76 ($\text{Ar-CH}_2\text{-NH}$), 28.64 ($\text{CH}_3\text{-tBu}$).

HR-MS (ESI): $[\text{M}+\text{Na}]^+$ calc.: 621.2755, found: 621.2763.

FT-IR (ATR, cm^{-1}): 3336 (br, w), 2921 (w), 1702 (m), 1676 (m), 1610 (m), 1563 (m), 1529 (m), 1434 (m), 1380 (vs), 1250 (m), 1144 (m), 1113 (m), 844 (s).

14-((5Z,8Z,11Z,14Z)-icosa-5,8,11,14-tetraenamido)-N-(4-(6-(pyrimidin-2-yl)-1,2,4,5-tetrazin-3-yl)benzyl)-3,6,9,12-tetraoxatetradecanamide (**4**)



tert-Butyl (3-oxo-1-(4-(6-(pyrimidin-2-yl)-1,2,4,5-tetrazin-3-yl)phenyl)-5,8,11,14-tetraoxa-2-azahexadecan-16-yl)carbamate (**3**) (66.0 mg, 0.1103 mmol) was solved in 1.15 mL DCM and 0.3 mL TFA was added. After 45 min the solvent was removed *in vacuo* and the resulting residue was used in the next step without further purification.

Arachidonic acid (54.6 μ mol, 166 μ mol, 1.5 eq.) was dissolved in 0.7 mL dry DMF and HATU (50.3 mg, 132 μ mol, 1.2 eq.), HOBT (44.7 mg, 331 μ mol, 3 eq.) and DIPEA (56,3 μ L, 332 μ mol, 3 eq.) were added. After 10 min the deprotected amine (55.0 mg, 110 μ mol, 1 Äquiv.), dissolved in 0.6 mL dry DMF, was added and the reaction was steered for 2h at RT. The reaction was diluted with DCM and washed with saturated NH_4Cl -solution. After drying of the combined organic phases over MgSO_4 and removing of the solvent *in vacuo*, the residue was purified by column chromatography (silica, *i*Hex/EtOAc, 1:1 \rightarrow DCM/EtOAc/MeOH, 10:10:1). **4** was received as violet oil (39,6 mg, 50,6 μ mol, 46%).

$R_f = 0.72$ ($\text{CH}_2\text{Cl}_2/\text{EtOAc}/\text{MeOH}$, 2:2:1).

$^1\text{H-NMR}$ (600 MHz, CDCl_3): δ [ppm] = 9.11 (d, $^3J = 4.8$ Hz, 2H, C- H_{arom}), 8.67 (d, $^3J = 8.4$ Hz, 2H, 2x $\text{C}3'$ - H_{arom}), 7.59 – 7.54 (m, 1H, C5- H_{arom}), 5.43 – 5.23 (m, 8H, 8x CH), 4.61 (d, $^3J = 6.2$ Hz, 2H, Ar- CH_2 -NH), 4.11 – 4.02 (m, 2H, C=O- CH_2 -O), 3.73 – 3.36 (m, 18H, tetraethylene glykole 8x CH_2 , CH_2 -NH), 4.11 – 4.02 (m, 2H, C=O- CH_2 -O), 3.73 – 3.36 (m, 18H, tetraethylene glykole 8x CH_2 , CH_2 -NH), 2.82 – 2.72 (m, 6H, 3xC- $\text{H}_{2\text{arach}}$), 2.18 – 2.12 (m, 2H, $\text{CH}_{2\text{arach}}$), 2.09 – 1.99 (m, 4H, 2xC-

H_{2arach}), 1.67 (q, ³J = 7.5 Hz, 2H, C-H_{2arach}), 1.37 – 1.20 (m, 6H, 3xC-H_{2arach}), 0.86 (t, J = 7.0 Hz, 3H, C-H_{3arach}).

¹³C-NMR (100 MHz, CDCl₃): δ [ppm] = 173.38 , 170.64, 164.54, 163.27, 159.72 (C_q), 158.64 (2xC_{arom}), 129.35 (CH), 129.33 (2xC), 128.90, 128.81, 128.74, 128.43, 128.38, 128.06, 127.72 (7xCH), 126.95, 122.75 (C_{arom}), 71.30, 70.65, 70.60, 70.47, 70.34, 70.13 (Tetraethylglykol 8xCH₂), 42.73 (CH₂-NH), 39.40, 36.21 (C_{arach}), 31.72 (C_{arach}), 29.92 (C_{arach}), 27.43 (C_{arach}), 26.91 (C_{arach}), 25.85 (C_{arach}), 25.83 (C_{arach}), 25.74 (C_{arach}), 22.79 (C_{arach}), 14.30 (C_{arach}).

HR-MS (ESI): [M+H]⁺ calc.: 785.4709, found: 785.4727.

FT-IR (ATR, cm⁻¹): 3311 (m), 2923 (s), 1555 (s), 1413 (s), 1103 (s).

Click chemistry of norbornene-containing hCA with anandamide tetrazine. MSNs (MSN-phSA, 0.5 mg) were loaded in 500 μL of calcein solution (1 mM) for 1 h. The loaded particles were collected by centrifugation (14,000 rpm, 16,837 rcf, 4 min) and 500 μL HBSS buffer solution was added. After addition of 0.5 mg norbornene-containing hCA the particles were redispersed and stirred for 1 h. Then, 5 μg anandamide tetrazine (DMSO stock solution, 2 mg/mL) were added and stirred for 1 h respectively. The particles were thoroughly washed with HBSS buffer (4 times), collected by centrifugation (5,000 rpm, 2,200 rcf, 4 min, 15 °C), and finally redispersed in 500 μL HBSS buffered solution.

Further Characterization

MSNs containing thiol-functionality exclusively at the external particle surface (sample MSN-SH) were established following a previously described delayed co-condensation approach.^[1] In a second step, benzene sulfonamide (phSA) groups were covalently attached to the silica

nanoparticles via a short bifunctional crosslinker (maleimide-C₆-NHS) at mild reaction conditions (sample MSN-phSA). After cargo loading, the enzyme CA was added to the buffered particle solution (pH 7.4). The formation of the inhibitor-enzyme complex (phSA-CA) leads to a dense coating at the external particle surface (MSN-phSA-CA).

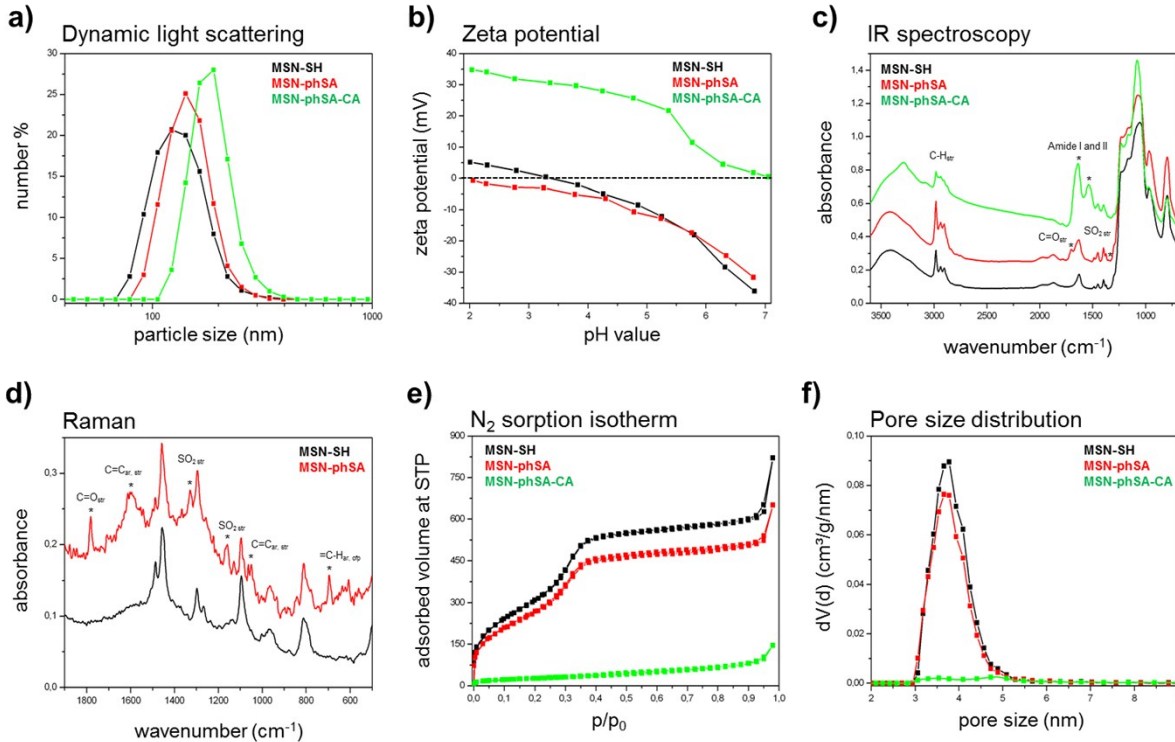


Figure S1: Characterization of multifunctional MSNs. a) Dynamic light scattering (DLS), b) zeta potential measurements, c) infrared (IR) spectroscopy data, d) Raman spectroscopy data, e) nitrogen sorption isotherms, and f) DFT pore size distribution of the MSNs. MSN-SH (black), MSN-phSA (red) and MSN-phSA-CA (green).

Dynamic light scattering (DLS) measurements showed the size distribution of the functionalized MSNs to be narrow and around 150 nm (Figure S1a), implying excellent colloidal stability after all functionalization steps. The surface charge of silica nanoparticles, measured as the zeta potential, changed due to the stepwise attachment of organic moieties (Figure S1b): The isoelectric point (IEP) of MSN-SH (pH 3.6) was shifted to a more acidic pH value (< 2) for MSNs containing the benzene sulfonamide groups on the outer surface. The tendency for sulfonamide

groups to be protonated is relatively low due to the stabilizing resonance effect, which leads to the increase in negative surface charge (predominantly influenced by silanol content). After attachment of the carbonic anhydrase, a drastic increase of the zeta potential was observed resulting from amino acid residues that can be easily protonated - such as arginine, histidine and lysine - on the surface. IR data for all samples showed typical vibrational modes of the silica framework between 780 and 1300 cm^{-1} (Figure S1c). MSNs containing the benzene sulfonamide groups showed additional modes for C=O stretching vibrations at 1700 and 1627 cm^{-1} and a peak of weak intensity at 1340 cm^{-1} , which belongs to the typical asymmetric SO_2 stretching vibration modes of the sulfonamide groups. For the sample MSN-phSA-CA, amide vibrations (Amide I: 1639 cm^{-1} , C=O stretching vibration; Amide II: 1535 cm^{-1} , N-H deformation and C-N stretching vibration) of high intensity were observed; these are typical for proteins. Raman spectroscopy provided data complementary to IR spectroscopy. In Figure S1d a more detailed view of the spectra for MSN-SH and MSN-phSA in the range between 1900 and 600 cm^{-1} is depicted and various additional bands (*) were observed for the benzene sulfonamide-functionalized particles. (data for MSN-phSA-CA not shown, for full range Raman spectra see Figure S4). Nitrogen sorption measurements show type IV isotherms for MSN-SH and MSN-phSA, confirming mesoporosity of the silica nanoparticles. Relatively high surface areas (up to 1200 m^2/g) and pore volumes (0.8 cm^3/g) were observed for MSN-SH and MSN-phSA (Table S1).

Table S1: Porosity parameters of functionalized MSNs.

Sample	BET surface area (m^2/g)	Pore volume ^a (cm^3/g)	DFT pore size ^b (nm)
MSN-SH	1170	0.83	3.8
MSN-phSA	1004	0.72	3.7
MSN-phSA-CA	99	0.07	-

^aPore volume is calculated up to a pore size of 8 nm to remove the contribution of interparticle porosity.
^bDFT pore size refers to the peak maximum of the pore size distribution.

Importantly, the DFT pore size distribution (Figure S1f) was not affected by the attachment of the benzene sulfonamide linkers and no incorporation of organic groups inside the mesopores was observed. The attachment of the bulky enzyme carbonic anhydrase resulted in a drastic reduction of surface area and pore volume for sample MSN-phSA-CA. Thus, the carbonic anhydrase enzymes were able to efficiently block the mesopores even towards the access of nitrogen molecules. We observed no pore size distribution for MSN-phSA-CA in the range between 2 and 9 nm. This confirms the successful synthesis of carbonic anhydrase-coated MSNs via benzene sulfonamide linkers.

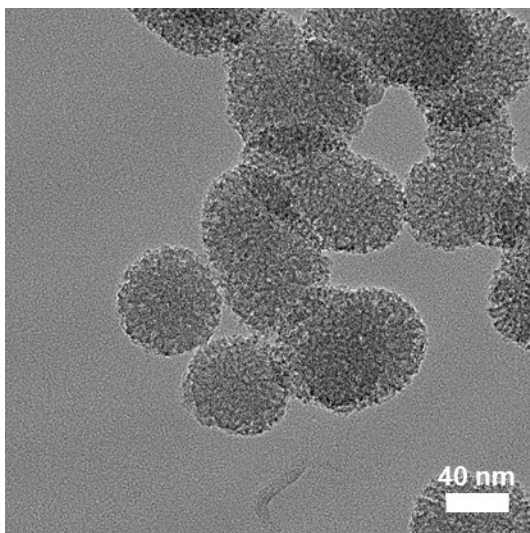


Figure S2: Transmission electron micrograph of thiol-functionalized MSNs (MSN-SH).

TEM images of thiol-functionalized MSNs are depicted in Figure S2 and display mostly spherically shaped particles with a radially disposed worm-like structure of the mesopores. The

mesoporous structure is also confirmed by the first-order reflection of the mesoporous material observed with small-angle X-ray diffraction (XRD) (Figure S3).

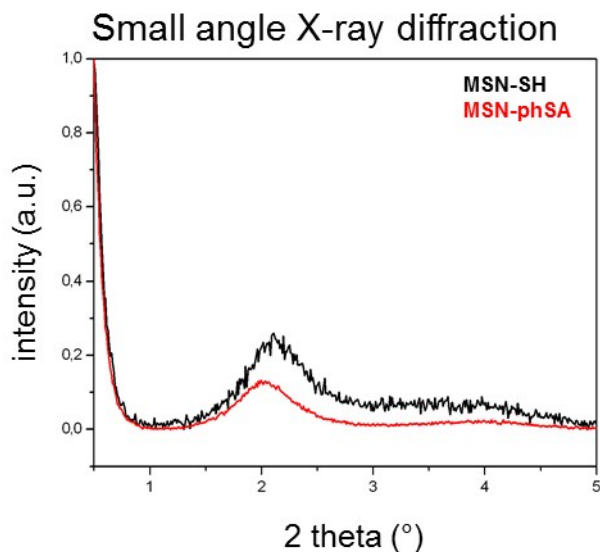


Figure S3: Small-angle X-ray diffraction pattern of MSN-SH (black) and MSN-phSA (red).

Full-range Raman spectra are shown in Figure S4. The sharp band at 1780 cm^{-1} can be assigned to the carbonyl stretching vibration of the diacylamine group of the maleimide residue that is covalently attached to the thiol groups of the MSN surface. The presence of phenyl groups is confirmed by characteristic bands of aromatic C=C stretching vibrations (1600 cm^{-1} and 1055 cm^{-1}) and aromatic =C-H out-of-plane deformation vibrations (693 cm^{-1}). The broadening of the signal at 1600 cm^{-1} can be assigned to a partial overlap by amide II vibration modes. The bands at 1326 and 1156 cm^{-1} are related to the characteristic asymmetric and symmetric stretching vibrations of the sulfonamide group, respectively.

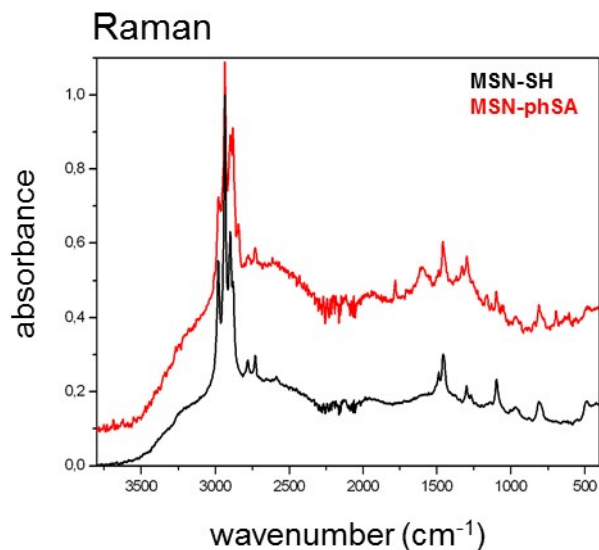


Figure S4: Raman spectroscopy data of functionalized MSNs. MSN-SH (black) and MSN-phSA (red). For clarity reasons, the spectra are shifted along the y-axis by 0.1 units. Measurements were performed at an excitation wavelength of 633 nm.

The amount of attached organic moieties on the MSNs was investigated by thermogravimetric analysis, showing an additional weight loss of about 14 % after attachment of CA (TGA, Figure S5). MSN-phSA particles show an additional weight loss of 3 % in the range between 130 and 900 °C due to the attachment of the benzene sulfonamide linker and enzyme-coated MSNs (MSN-phSA-CA) feature a relatively high additional weight loss compared to sample MSN-SH (+14 % at 900 °C). Apparently, degradation of the carbonized enzymes occurs only at very high temperatures, and is not even finished at 900 °C. This was already observed before for thermogravimetric analysis of enzyme-coated MSNs.

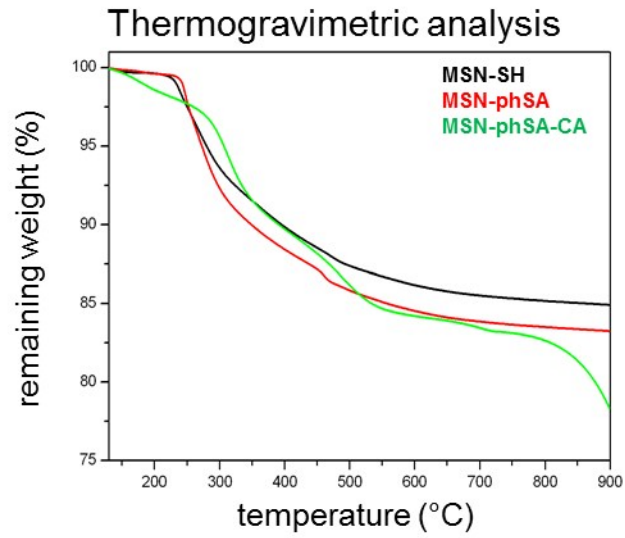


Figure S5: Thermogravimetric analysis of MSN-SH (black), MSN-phSA (red), and MSN-phSA-CA (green).

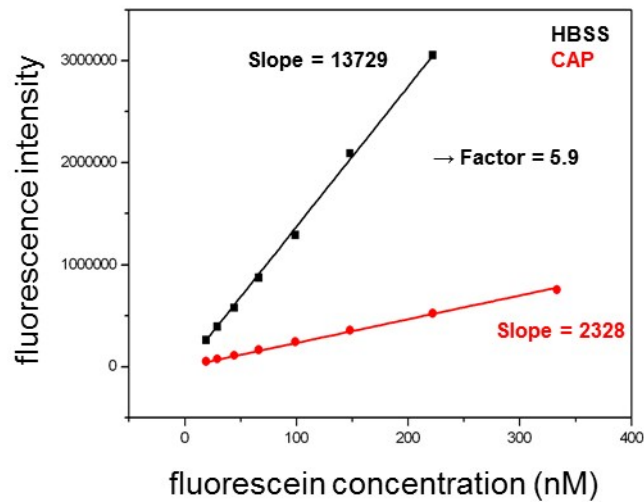


Figure S6: Calibration curves of fluorescein at pH 7.4 (HBSS buffer, black curve) and pH 5.5 (CAP buffer, red curve).

The enzyme activity assay investigates the hydrolysis in TRIS-buffered solution of a chromogenic substrate (p-nitrophenyl acetate, NPA) in the presence of the enzyme, generating nitrophenol.

UV-Vis spectroscopy is used to measure the resulting absorption maximum at 400 nm. Figure S7 shows the resulting curve for the non-catalyzed (no carbonic anhydrase) reaction, which can be taken as baseline. The slight slope for this curve is due to the hydrolysis rate of the pure substrate in aqueous solution in the absence of catalytic enzymes. In the presence of 100 nM enzyme (non-inhibited) the maximum conversion of the substrate can be obtained. A slight decrease in conversion efficiency can be observed upon addition of 50 μg of MSN-SH particles due to marginal reduction of enzyme activity in the presence of silica nanoparticles. We assume that this effect corresponds to minor unspecific attachment of the carbonic anhydrase to the silica nanoparticles causing blocking of the active sites to some extent. In comparison, the addition of inhibitor-containing particles (MSN-phSA) causes a significant decrease of the slope of the resulting curve. This proves a specific formation of the inhibitor-enzyme complex at the external surface of the silica nanoparticles. Thus we have shown conclusively that the sulfonamide-functionalized MSNs are able to bind the enzyme carbonic anhydrase. At neutral pH values, the enzyme is specifically attached to the sulfonamide-functionalized particle surface resulting in an inhibition of the enzyme's active site. This leads to a drastic decrease in enzyme activity.

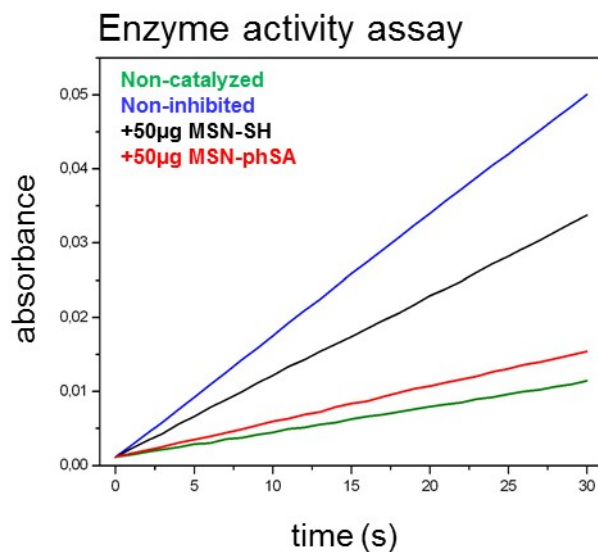


Figure S7: Enzyme activity assay of CA catalyzing the hydrolysis of the chromogenic substrate p-nitrophenyl acetate measured by UV-Vis spectroscopy (absorbance at 400 nm). Non-catalyzed (green) and non-inhibited (blue) reaction and after addition of MSN-SH (black) or MSN-phSA (red).

In order to verify the fate of our drug delivery vehicles ending up in acidic cell compartments, co-localization experiments with labeled MSNs and endosomes or lysosomes were performed. Simultaneous with particle incubation, the HeLa cells were transfected with a BacMam reagent in order to express different fusion-constructs of green fluorescent protein (GFP) and early/late endosome or lysosome markers, respectively. After 24 h of incubation with fluorescently labeled nanoparticles, almost no co-localization (yellow) between early endosomes and MSNs could be observed, as can be seen in Figure S8a. In contrast, multiple yellow spots indicating co-localization between GFP (green) and MSNs (red) were clearly visible in the case of late endosomal and lysosomal staining after 21 h (Figure S8b/c, denoted by arrows). This shows that the localization of our nanocarriers in an acidic compartment is crucial to initiate cargo release.

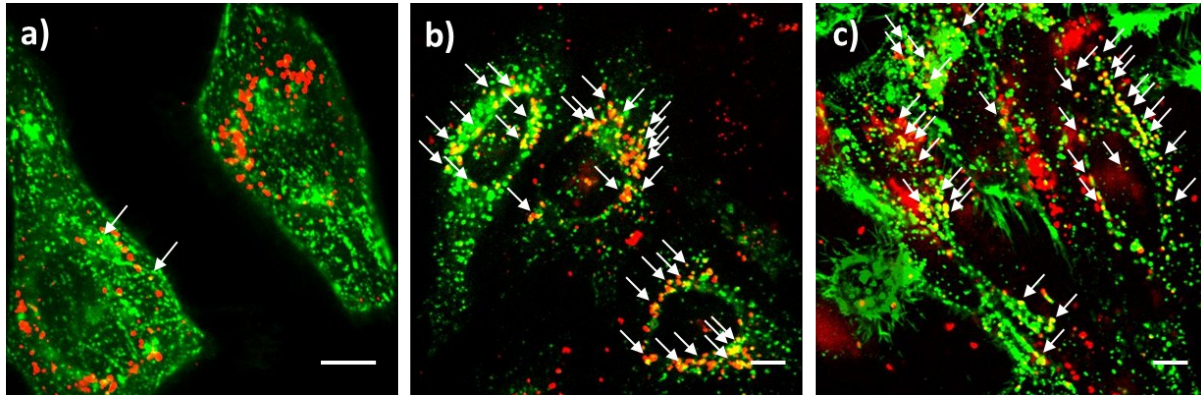


Figure S8: Fluorescence microscopy of HeLa cells incubated with Atto 633-labeled MSN-phSA-CA (red) after a) 24 h on GFP-early endosome (green) tagged cells, b) 21 h incubation on GFP-late endosome (green) tagged cells, and c) 21 h on GFP-lysosome (green) tagged cells. Co-localization (yellow) could be primarily observed for late endosomes and lysosomes (indicated with arrows) suggesting that the multifunctional MSNs are located in acidic compartments after endocytosis. The scale bar represents 10 μm .

Stem Cell targeting

To test targeting of anandamide functionalized particles neural stem cells were treated with anandamide functionalized particles. As control, cells were pretreated with free anandamide-tetrazine and incubated with anandamide particles after 2 h of pretreatment. Another control was performed with control particles without anandamide functionalization. After two hours of particle incubation all cells were washed with medium. Already a few hours after incubation anandamide-particles were observed to stick to the cells in large amounts whereas particles without anandamide did not show this behavior. After 24 h anandamide-targeted particles were successfully taken up into the cells. Cells that were incubated with control particles or preincubated with anandamide did not show as much particle uptake (Fig. S9).

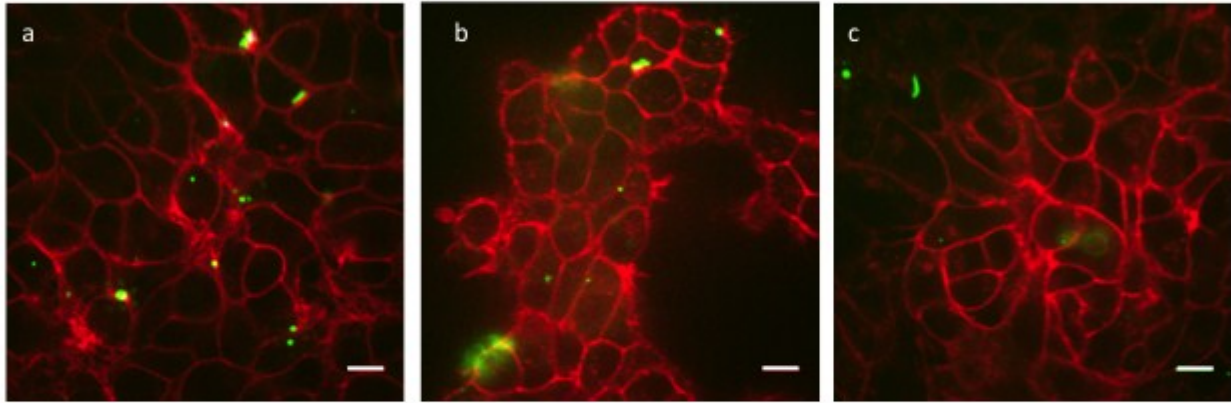


Figure S9: Fluorescence microscopy of neural stem cells incubated with calcein-labeled MSN-phSA-CA (green) after 24h a) incubated with anandamide-targeted MSN-phSA-CA, b) pretreated with free anandamide-tetrazine and incubated with anandamide targeted MSN-phSA-CA afterwards c) incubated with control MSN-phSA-CA without anandamide. Cell membranes are stained with cell mask deep red. The scale bar represents 10 μm .

A431 cell targeting

To test the targeting of cannabinoid receptors with anandamide-functionalized particles on A431 cells, the receptors were either blocked or free corresponding to the folate-based experiments. The functionality was evaluated in a receptor competition experiment. For this purpose, A431 cells were seeded in ibidi 8 well μ -slides (ibiTreat, ibidi) at a concentration of 10000 cells and 300 μl DMEM medium per well. 24h after seeding, one part of the A431 cells was pre-incubated with 10 μL of an inhibitor mixture (1 mg/mL anandamide-tetrazine in DMSO, 1 mg/mL folic acid), to block the receptors, for 4 h at 37 $^{\circ}\text{C}$ under a 5% CO_2 humidified atmosphere. Then the A431 cells were incubated with 5 μg MSN-phSA-CA-Anandamide particles for 3 h at 37 $^{\circ}\text{C}$ under a 5% CO_2 humidified atmosphere. For staining the cell membrane, the

cells were incubated with CellMask orange (0.05%) for 1 min. The cells were washed three times with PBS, fresh medium was added and subsequently the cells were imaged. Clearly an enhanced receptor-mediated cell uptake can be seen when the cannabinoid receptors are available on the cell surface.

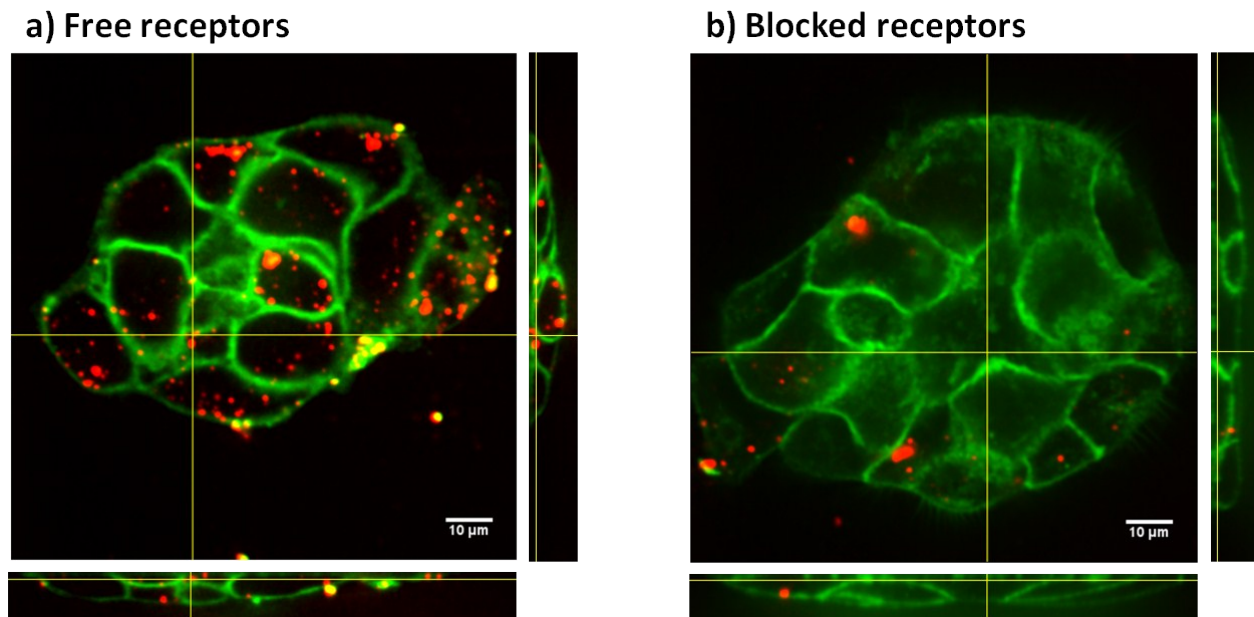


Figure S10: Fluorescence microscopy of A431 cells incubated with Atto633-labeled MSN-phSA-CA (red) after 3h a) incubated with anandamide-targeted MSN-phSA-CA, b) pretreated with free inhibitors and incubated with anandamide targeted MSN-phSA-CA afterwards. Cell membranes are stained with CellMask orange (green).

Cell viability studies

For MTT-Assays we seeded 5000 HeLa cells per well containing 100 μL of the respective medium and treated them with MSN-phSA-CA and MSN-phSA-CA+AmD 24h after seeding. After 24 h of incubation the cells were washed three times with PBS buffer. 100 μL of 3-(4,5-dimethylthiazol-2-yl)-2,5-diphenyltetrazolium bromide (MTT, 0.5 mg/mL in DMEM) was added to each well of the nanoparticle-treated cells and incubated for further 2 h. Unreacted MTT and medium were

removed and the 96-well plates were stored at -80 °C for at least 1 h. Then, 100 μ L DMSO was added to each well. The absorbance was read out by a Tecan plate reader. All studies were performed in triplicates.

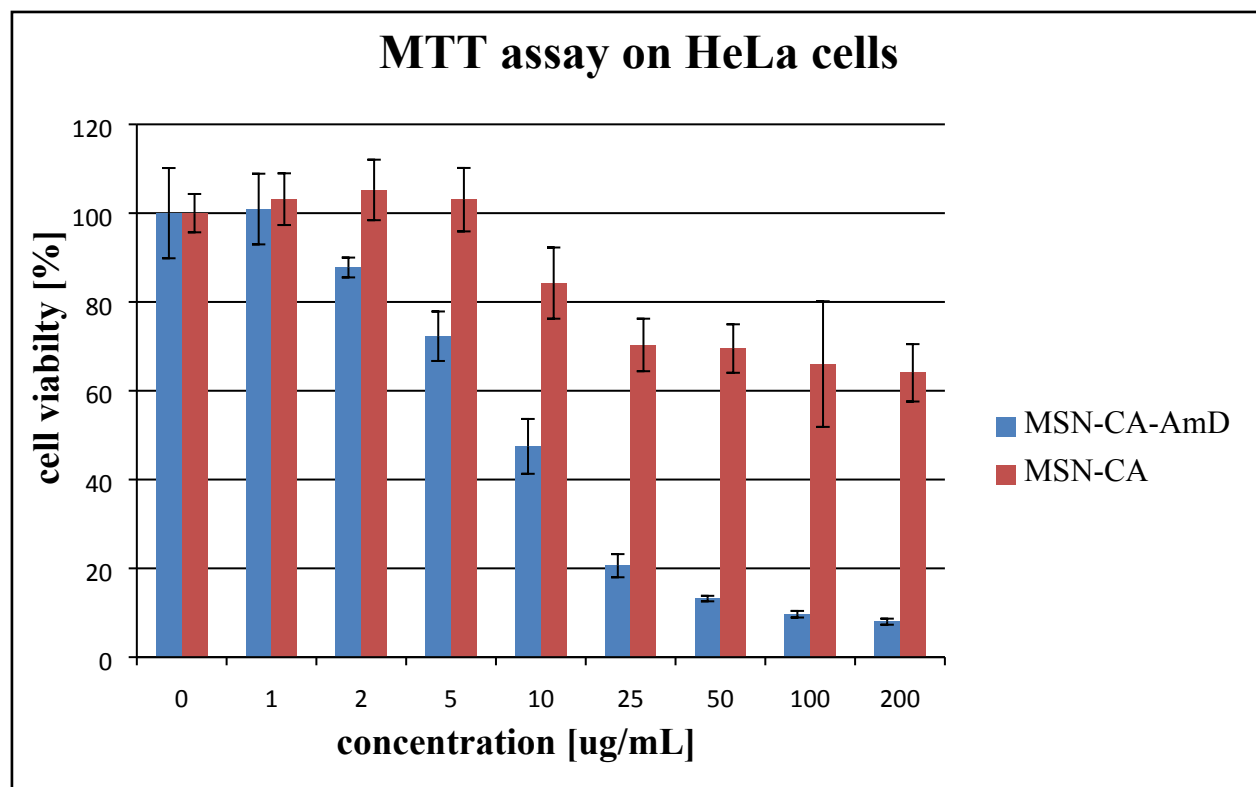


Figure S11: MTT assay on HeLa cells with MSN-phSA-CA and MSN-phSA-CA+AmD (according to Figure 5). Incubation time was 24 h.

References

- [1] V. Cauda, A. Schlossbauer, J. Kecht, A. Zürner, T. Bein, *J. Am. Chem. Soc.* **2009**, *131*, 11361.